Available online at www.sciencedirect.com

ScienceDirect

Ceramics International 39 (2013) 9583–9590

CERAMICS INTERNATIONAL

www.elsevier.com/locate/ceramint

# Design of ceramic tiles with high solar reflectance through the development of a functional engobe

Chiara Ferrari*, Antonio Libbra, Alberto Muscio, Cristina Siligardi

*Dipartimento di Ingegneria "Enzo Ferrari", Università di Modena e Reggio Emilia, Via Vignolese 905/A, 41125 Modena, Italy*

Received 21 February 2013; received in revised form 14 May 2013; accepted 18 May 2013
Available online 28 May 2013

**Abstract**

Roofing solutions with high capacity to reflect incident solar radiation, the so-called cool roofs, can provide an effective answer to summer overheating of either individual buildings or whole urban areas. Nowadays, commercial cool roof products are mainly represented by organic membranes and coatings, but ceramic tiles can offer an interesting alternative or complement in view of their high durability. This work presents the procedure through which a traditional white engobe and a glazed tile with high solar reflectance are developed by the introduction of suitable raw materials and pigments, in the perspective of production by commonly used industrial processes. The solar performance was checked for both light and dark supports and for different engobe thicknesses up to 250 μm; the estimated solar reflectance values were correlated with surface properties such as microstructure, mineralogical composition, and roughness. The best performing engobe, applied as a 200 μm layer, improved solar reflectance of the sample up to 0.90. Three different glazes were then applied on engobed samples and were found to slightly affect the reflectance and improve the resistance to mechanical stress or weathering. A white gloss glaze was found to be the best performing one in terms of solar reflectance.


*Keywords:* Cool roof; Cool tile; Engobe; Glazed tile; Solar reflectance

## 1. Introduction

Limiting summer overheating of buildings and mitigating the urban heat island effect are the principles behind cool roofs [1,2], roofing solutions with high capacity to reflect incident solar radiation. Among direct benefits of lower building overheating there are lower costs for air conditioning and greater comfort inside buildings, as well as lower structural stress, chemical or physical material degradation and roof maintenance cost; among indirect benefits, coming from mitigation of the urban heat island effect, there are smog reduction, public health and also energy benefits such as peak energy saving and grid stability [1–7]. The cool roof concept has also evolved into cool colors [8,9], coating solutions which combine esthetic requirements with material functionality.

The cool roof market is nowadays dominated by organic membranes and coatings, which can reach very high values of solar reflectance ($\rho_{sol}$=0.80/0.90 for white products). The solar reflectivity spectrum of organic coatings, however, often shows a sharp decrease as one moves from the visible range in the near infrared (NIR). On the other hand, white ceramic tiles are generally characterized by slightly lower solar reflectance values ($\rho_{sol}$=0.60/0.80) [10], but their reflectivity spectrum, in contrast to organic materials and coatings, can show a high and nearly flat trend in the NIR [11,12]. When a given reflectivity spectrum in the visible range is required to obtain a certain non-white color, a true cool color product can be achieved by maximizing the reflectivity in the NIR and, in this context, ceramic tiles can provide an interesting alternative or complement to organic materials and coatings.

A traditional porcelain stoneware tile is made by at least three different layers: a ceramic support, a thin engobe application and one or more glaze applications. This is the same structure of advanced cool color products [8], consisting of a support material, a high reflectance basecoat deposited onto the support surface, and an IR-transparent topcoat placed onto the basecoat. Solar radiation is allowed to pass through the topcoat, so that infrared radiation is reflected from the basecoat, crosses again the topcoat and eventually leaves the

*Corresponding author. Tel.: +39 059 205 6282; fax: +39 059 205 6243.
*E-mail address:* chiara.ferrari@unimore.it (C. Ferrari).

0272-8842/$ - see front matter 
http://dx.doi.org/10.1016/j.ceramint.2013.05.077

Table 1
Engobes composition (wt%).

| Sample | Set 1 | | | | | Set 2 | | | |
|---|---|---|---|---|---|---|---|---|---|
| | A2 | B2 | C2 | D2 | N2 | A3 | B2 | C3 | D3 |
| Na feldspar | 45 | 30 | | | 30 | 45 | 32 | | |
| Recycled glass | | | 30 | 45 | | | | 30 | 43 |
| Nepheline syenite | | | | | 15 | | | | |
| Alumina | 10 | 25 | 25 | 10 | 10 | 9 | 25 | 23 | 10 |
| Quartz | 10 | 15 | 15 | 10 | 10 | 11.5 | 16 | 14 | 10 |
| Kaolin | 10 | 10 | 10 | 10 | 10 | 10 | 10 | 10 | 10 |
| $ZrSiO_4$ | 10 | 10 | 10 | 10 | 10 | | | | |
| $TiO_2$ | | | | | | 4.4 | 4.8 | 4.3 | 4.1 |
| White clay | 15 | 10 | 10 | 15 | 15 | 15 | 15 | 10 | 15 |
| Sodium Tripolyphosphate | 0.2 | 0.2 | 0.2 | 0.2 | 0.2 | 0.2 | 0.2 | 0.2 | 0.2 |
| Carboxymethyl cellulose | 0.2 | 0.2 | 0.2 | 0.2 | 0.2 | 0.2 | 0.2 | 0.2 | 0.2 |

material, whereas the optical color is obtained by the visible reflection/absorption spectrum of selective pigments dispersed in the topcoat [13,14].

Among ceramic products, clay roof tiles were previously studied [10–12] concerning both natural ageing and organic coatings formulation, and one of the main faced issues was related to the relatively unnatural aspect given by the deposition of paints on roof tiles, if compared with the natural terracotta aspect of these covering materials. Porcelain tiles seem not to be properly considered as a cool materials since when Libbra et al. [11] started to analyze either some commercial products or experimental glazed tiles developed at EELab, in order to optimize both substrates and pigmented glazes made of common and cheap raw materials.

In this work we focused on a completely new product, and not just a cool coating, in which we considered as support the traditional ceramic body, the basecoat is represented by the engobe and the NIR-transparent topcoat is the glaze, and all components are managed in the framework of a conventional production process of the ceramic industry.

The engobe is a very important step in the tile production process because this thin layer between the ceramic support and the glaze prevents reactions between chromophore impurities, ensures a good opacity and a high whiteness degree, improves the dilatometric match between the support and the glaze. It also improves impermeability and, consequently, it prevents staining due to colored solutions that may come in contact with the fired tiles. It is made by several raw materials such as ball-clay, which provides plasticity, various frits (30–40%) helping the glassy phase formation and, sometimes, feldspar and quartz, which allow control of mixture melting point and thermal expansion coefficient. In order to improve the engobe whiteness, other raw materials can be added.

Glazes are vitreous coatings applied onto the exposed tile surface in order to make it waterproof, tougher and more resistant to dirt, as well as to improve its esthetic aspect. Glaze composition is extremely variable and complex, consisting mainly of frits and other additional components in variable percentages such as kaolin, ball-clay, bentonite, opacifiers, pigments, or additives to control the glaze rheology during application [15].

A main aim of this work is to design an inorganic engobe with high solar reflectance, as well as to investigate the glaze influence on the reflectance.

A white cool roof material can be obtained in case of white engobe and non-pigmented glaze, whereas cool color ceramic coatings can be derived by adding proper pigments with selective absorption in the visible-NIR spectrum to the glaze. With regard to the industrial process, the study is carried out using the same production methods and the same average composition of traditional porcelain stoneware tiles, products of Italian manufacture worldwide appreciated for their special features, first of all for resistance to sun, rain and frost.

At this first stage of the work, the attention is focused only on white pigments, in order to obtain the highest reflectivity throughout the solar spectrum. Among the different white pigments currently in use in the ceramic industri, two pigment have been selected to be included in the formulation of an engobe with high and flat reflectivity spectrum. The two pigments are alternative but very differen one from the other. Thereafter, three different types of glaze were applied onto a tile support coated with the best performing engobe, in order to check how solar reflectance is affected by the glaze itself.

## 2. Materials and methods

### 2.1. Sample preparation

The engobes were prepared according to formulations detailed in Table 1 Two sets of formulations were considered, the first set made of samples characterized by the presence of $ZrSiO_4$ (64.00% $ZrSiO_4$+$HfO_2$, 35.2% $SiO_2$, 0.40% $Al_2O_3$, 0.25% $TiO_2$, 0.10% $Fe_2O_3$) while $TiO_2$ (92.7% $TiO_2$, 0.73% $SiO_2$, 0.40% $Al_2O_3$, 0.98% $Fe_2O_3$, 5.19% others) is the pigment introduced into the second set of samples. In the second set, $ZrSiO_4$ is replaced by the same number of moles of $TiO_2$. The two selected pigments, $ZrSiO_4$ and $TiO_2$, are commercial and relatively cheap products widely used in traditional ceramic formulations. The main difference between them is that both ones are characterized by high refraction index $n$, but the $n$ value of $ZrSiO_4$ is around 1.94 while the $n$ value of $TiO_2$ is around 2.52 [16].

To ensure that the granulometric distribution of the two pigments is the same and it does not affect the optical properties of the raw material, a granulometric distribution analysis was performed on both raw materials using a particle size analyzer [17] (Table 2).

Sample with label N2 is characterized by the presence of Nepheline Syenite (60.14% $SiO_2$, 23.5% $Al_2O_3$, 92.7% $Fe_2O_3$, 16.38% others) as partial replacement of Na Feldspar (68.9% $SiO_2$, 19.30% $Al_2O_3$, 0.02% $Fe_2O_3$, 0.02% $TiO_2$, 11.76% others). In both formulation sets, samples with label starting with C or D are characterized by a high amount of recycled glass. Entering in detail, a recycled boric glass made of 73.40% $SiO_2$, 6.30% $Al_2O_3$, 0.87% $K_2O$, 6.62% $Na_2O$, 1.10% CaO, 10.40% $B_2O_3$, and 1.01% BaO was used. The granulometric distribution analysis of the glass powder returned an average diameter of 87 μm at $D_{90}$.

Table 2
Pigment granulometric distribution.

| | $D_{10}$ (μm) | $D_{50}$ (μm) | $D_{90}$ (μm) |
|---|---|---|---|
| $ZrSiO_4$ | 0.44 | 1.70 | 4.76 |
| $TiO_2$ | 0.47 | 2.23 | 4.49 |

The above described raw materials, selected among the most widely used in the Italian ceramic district according to their optical properties, were mixed with Kaolin (49.60% $SiO_2$, 36.40% $Al_2O_3$, 0.12% $Fe_2O_3$, 0.05% $TiO_2$, 13.83% others), White clay (52.50% $SiO_2$, 31.70% $Al_2O_3$, 1.00% $Fe_2O_3$, 1.05% $TiO_2$, 13.75% others), Alumina (0.01% $SiO_2$, 99.4% $Al_2O_3$, 0.01% $Fe_2O_3$, 0.01% $TiO_2$, 0.58% others) and Quartz (96.20% $SiO_2$, 2.40% $Al_2O_3$, 0.12% $Fe_2O_3$, 0.05% $TiO_2$, 1.23% others).

Raw materials were poured in an alumina jar with the addition of 40 wt% of water and alumina milling balls having different diameters. After the milling process, the engobes presented a density of 1.53 g/mL. They were subsequently dried and wet sieved using the fraction passing though a 100 μm mesh sieve as a common practice, and then applied in two layers onto the ceramic support by means of an airbrush.

Two different types of tile were used as the ceramic support, shaped 30 cm × 30 cm, one white ($\rho_{sol}$=0.48) and the other one red ($\rho_{sol}$=0.37) in order to analyze the effect of the support color. Moreover, two, three and four layers of engobe were applied by an airbrush onto different red tiles, in order to verify the engobe opacity in the diverse conditions. Since the airbrush application is deeply influenced by the manual skill of the operator, the engobe thickness was measured in cross section by means of a SEM and it was quantified in about 150 μm for two airbrush applications, while it increases to about 200 μm with three applications and to about 250 μm with four applications. The sample weight was also checked after every engobe application to verify the amount of engobe applied onto the tiles.

All the samples were fired in an industrial roller kiln at the maximum temperature of 1195 °C for 6 min, in a cold to cold cycle which totally lasts 47 min.

The solar properties of all the engobed samples were eventually measured and three different commercial glazes, a transparent one, a commercial white gloss glaze and a commercial white matt glaze, were applied on the two best performing formulations, using either white or red ceramic supports. The investigation was aimed at analyzing the interaction of the glaze with the engobe and at understanding the behavior of the 'cool' engobe-glaze system. The glazes were obtained from different frits to promote the particular features of each glaze, with the addition of kaolin and other raw material to improve rheological behavior [15]. The glazed samples were also fired at the same conditions of unglazed engobed tiles.

### 2.2. Sample characterization

X-ray Diffraction (XRD) analysis was conducted using Cu Kα radiation limited to 40 kV and 25 mA and a gas proportional counter (X′pert PRO, Panalytical) in order to determine the mineralogical phases present in both the glaze or the engobe. XRD spectra were collected on the sample surface with a scanning rate of 0.1°/min for 2$\theta$ from 10° to 70°

A SEM analysis was performed by means of a scanning electron microscope (FEI XL-30), in order to investigate the surface of unglazed and glazed samples and study the engobe thickness influence on solar properties. In the thickness investigation, the analyzed samples were cut using a diamond cutter and then ground by SiC abrasive paper, followed by polishing with diamond paste (3 and 1 μm) and lapping oil. The samples were coated with a 10 nm thick gold layer using the sputtering technique.

A UV–vis–NIR spectrometer (Jasco V-670) with a 150 mm integrating sphere was used to measure the spectral reflectance of each sample, following the ASTM E903 Standard Test Method. More specifically, the solar reflectance value $\rho_{sol}$ of every analyzed surface was calculated by integrating over the range from 300 to 2500 nm the measured spectral reflectivity $\rho_\lambda$ (defined as the ratio of reflected part and total amount of incident radiation at the considered wavelength $\lambda$), weighted by the standard spectral irradiance of the sun at the earth surface, $I_{sol,\lambda}$ [$Wm^{-2}$ $nm^{-1}$]:

$$\rho_{sol} = \frac{\int_{300}^{2500} \rho_\lambda I_{sol,\lambda} d\lambda}{\int_{300}^{2500} I_{sol,\lambda} d\lambda} \quad (1)$$

Surface roughness allows understanding the level of soil resistance of a sample. A rougher surface usually retains more easily the dirt that is deposited on it. This causes deterioration of optical properties. The surface profile was analyzed with a roughness tester (Diavite DH-5 V1.50 with a DIAVITE 5478 tracer) that records the roughness along the length $L$ (4.8 mm), thus providing a profile from which the synthetic parameters that characterize the roughness itself are extracted. The three measured parameters are $R_z$, $R_{max}$ and $R_a$ [18]. $R_z$ is the distance between two straight lines parallel to the middle line drawn at distances equal to the average of the five highest peaks and the average of the five lowest valleys in the range of the length $L$. $R_{max}$ is the distance between two lines parallel to the middle line, the first tangential to the highest peak and the second tangential to the lower valley. $R_{max}$ is therefore the maximum of the profile irregularities. The roughness $R_a$ is a mean roughness value that, however, does not reveal the type of irregularity.

$$R_a = \frac{1}{L}\int_0^L |Y| dx \quad (2)$$

## 3. Result and discussion

### 3.1. XRD analysis

An XRD analysis was performed in order to more accurately classify, in qualitative terms, the mineralogical phases present in the engobes (Table 3). The diffraction analysis was performed on the engobed surface of the samples.

Among samples in Set 1, crystal structures of sample B2 are formed directly from the raw materials used in the engobe after heat treatment. As it can be seen on the table, during the firing process two new phases, Mullite and α-Cristobalite, formed as a consequence of the heat treatment. The crystalline phases in the sample result from the crystallization of the high percentage of frits introduced in the formulation and the heat treatment of raw materials. Sample C2 is also characterized by the presence of an amount of vitreous phase, given mainly by the 30 wt% of frits used into the formulation. An even stronger presence of vitreous phase occurs in sample D2 because of the high percentage of recycled glass employed into the formulation as replacement of Na Feldspar. Sample N2, instead, is characterized by a degree of cristallinity higher than C2 and D2 highlighted by the well defined peaks shape. This behavior is comparable to that of sample B2; and is caused by the mineralogical composition of sample N2: the percentage of recycled glass which was introduced in C2 and D2, is replaced by nepheline syenite and Na-feldspar.

Table 3
XRD semiquantitative analysis of unglazed samples.

| | Corundum | Quartz | Albite | Mullite | Cristobalite low | Zircon | Rutile | Anatase |
|---|---|---|---|---|---|---|---|---|
| B2 | ** | ***** | ** | ** | | *** | | |
| C2 | ** | *** | | | | *** | | |
| D2 | * | *** | | | | *** | | |
| N2 | * | **** | *** | * | | *** | | |
| B3 | ** | **** | ** | * | | | * | |
| C3 | ** | *** | | | | | * | * |
| D3 | * | ** | | | * | | * | * |

The behavior of samples in Set 2 (i.e. formulations B3, C3, or D3) can generally be assimilated to that of samples in Set 1. The main difference regards the presence of the crystalline phases formed from $TiO_2$ (Anatase and Rutile) in place of that formed from $ZrSiO_4$ (Zircon) in Set 1 samples. More specifically, the XRD analysis shows that the phase forming $ZrSiO_4$ is inert to heat treatment, while $TiO_2$ seems to be more reactive as two distinct crystalline phases are formed in samples C3 and D3 as a result of heat treatment of the engobe. The presence of cristobalite, in the sample D3, let us know that the duration of the firing cycle was not sufficient to conclude the crystallization of quartz considering that the rate of transition from quartz to Cristobalite exceeds the rate of quartz dissolution. [19]

### 3.2. SEM analysis

#### 3.2.1. Engobed unglazed samples

The morphological study is based on examination of the surface of the samples by SEM. Sample B2 (Fig. 1) presents a surface where raw materials seem almost incoherent. It appears that the high refractoriness of the formulation prevents cohesion of powders. Instead, sample C2 presents a surface which is significantly different. The presence of frits allow the formation of glassy phase binding the crystalline phases and contributing to a more effective consolidation. Sample D2, containing recycled glass as a replacement of Na Feldspar, is characterized by the presence of a glassy phase and presents a smooth surface, in which porosity is absent. In all SEM images of Set 1 samples, one can easily recognize the crystalline phase from $ZrSiO_4$ crystals completely surrounded by glass. Sample N2 presents a surface more similar to that of sample C2 due to

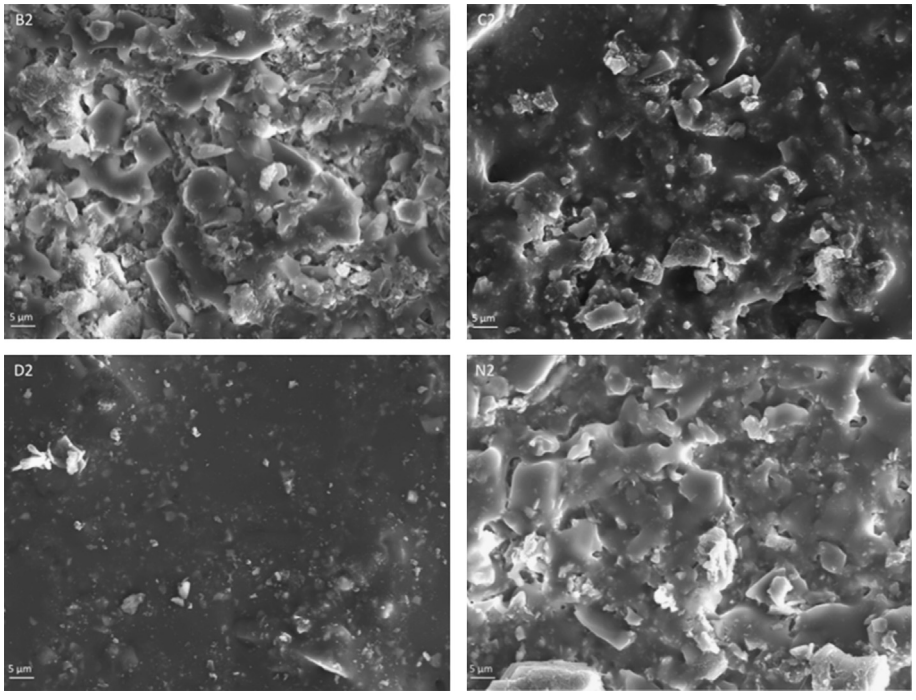


Fig. 1. Set 1 unglazed samples surface micrographs SED image 1000 × .

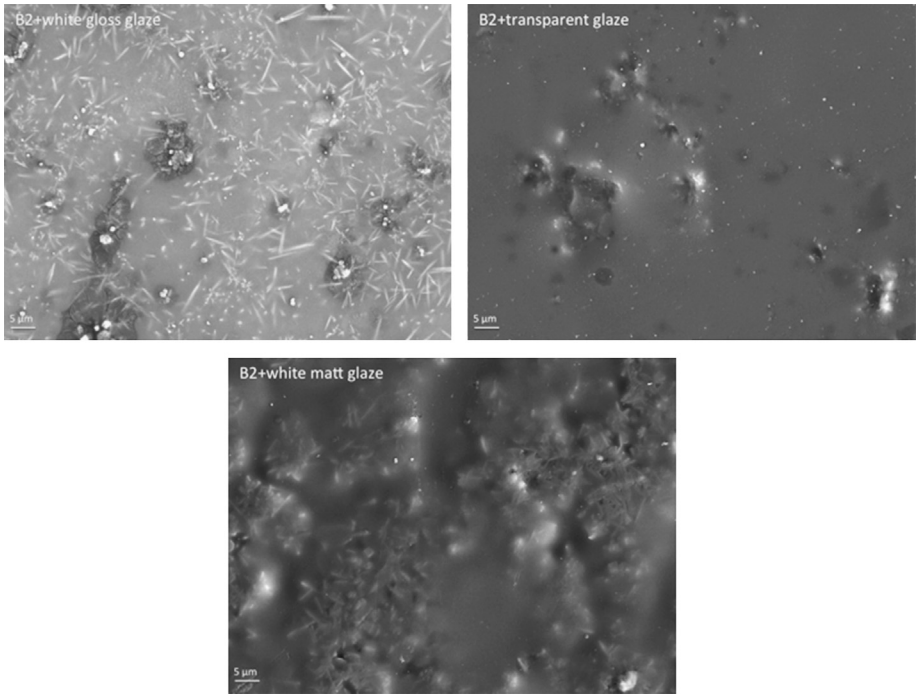


Fig. 2. B2 glazed samples surface micrographs SED image 1000 × .

the similar amount of the vitreous phase, that, in this case, is formed also thanks to thermal transformation of nepheline. With regard to samples in Set 2, a good overlap with the microstructure of corresponding samples in Set 1 can be observed, in perfect analogy with what occurs in the XRD analysis, and SEM images are therefore omitted.

### 3.3. Glazed samples

Fig. 2 shows how the surface of sample surface B2 looks like with the three different glazes (clockwise: white gloss glaze, transparent glaze, white matt glaze). A very interesting microstructure can also be observed on the surface of sample "B2 +white gloss glaze" applied, as $ZrSiO_4$ originates a crystallization with internal acicular (i.e. slender needle-like) crystals. As one can see, in "B2+transparent glaze" micrograph, the surface area is flat and smooth, thus allowing a shiny surface. To achieve this effect it is necessary that, at the formation temperature of the coating, the crystalline phases formed during the heating phase melt completely and subsequently do not crystallize during the cooling process. The last SEM image shows the surface of sample "B2+white matt glaze", where the presence of some crystals can again be observed. The matt effect on the surface depends on the type and quality of crystals in the coating, and the glaze component that originates such structures is nepheline. Generally speaking, a strong difference can be observed in SEM images between the three glaze types.

### 3.4. Roughness analysis

The roughness test was carried out on both sample B2 (Fig. 3) and sample C2 (Fig. 4). The extracted profiles are very similar; therefore one can assume that the microscopic surface defects evidenced by SEM analysis do not influence the results. Samples coated with transparent glaze and white gloss glaze have very similar profiles, as seen on the SEM cross section in Fig. 5.

The values of $R_a$ recorded for those samples are about 0.40 µm and 0.42 µm, respectively, while the roughness of the matt glaze is approximately doubled, with $R_a$ equal to 80 µm. A functional consideration can lead to the conclusion that the surfaces with less dirtying problems are the gloss ones as the pronounced roughness of the matt glaze gives a higher chance of dirt to lock into the surface asperities and reduce solar reflectance. Moreover, the white matt glaze has a lower soil resistance, and potentially higher maintenance cost. A correlation between surface roughness and solar properties seems also to exist because the white matt glaze has lower reflectivity in comparison with the white gloss glaze or the transparent glaze (Table 3). It should be noted, however, that samples with similar roughness like those with transparent glaze and glossy white glaze have different reflectance values, therefore it is not possible to directly correlate the roughness to the optical properties without taking into account the mineralogy of engobe and glaze.

### 3.5. Solar reflectance

Solar reflectance values, measured for both sets of engobed unglazed samples are shown in Table 4, where one data column is related to red ceramic support and the other one is related to white support. All the samples present interesting values ranging from $\rho_{sol}=0.63$ to 0.90 for the sample on the red support and from $\rho_{sol}=0.66$ to 0.90 for the engobes applied on the white support. Engobes sprayed onto the white

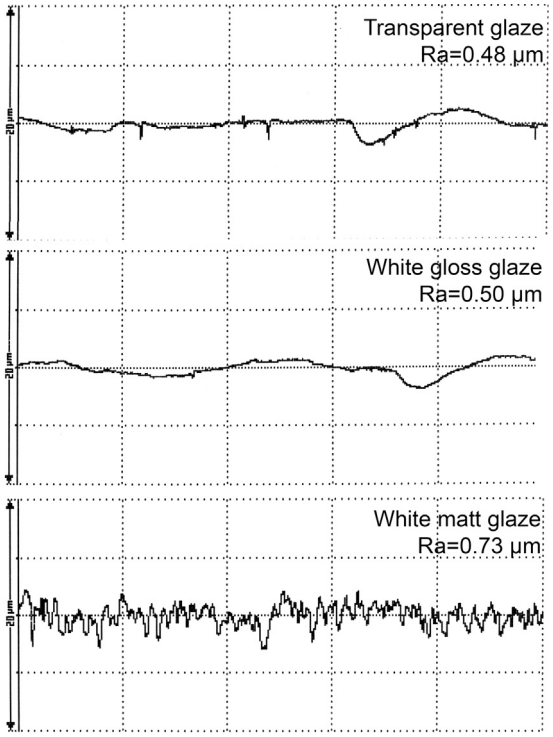


Fig. 3. Roughness profile of B2 glazed samples.

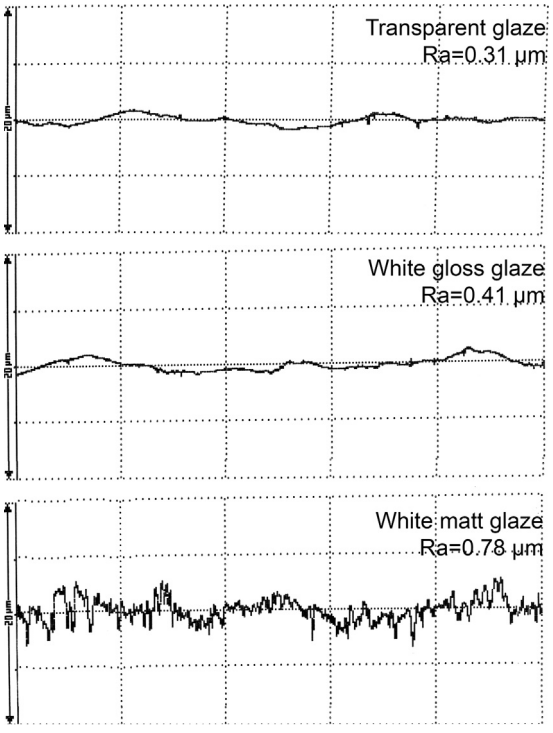


Fig. 4. Roughness profile of C2 glazed samples.

support are always better performing than those sprayed onto the red support.

In the first sample set (Set 1), samples with engobe composition B2, on both red and white supports, and samples with engobe composition C2, on white support, are the best performing ones, with solar reflectance as high as 0.90 and

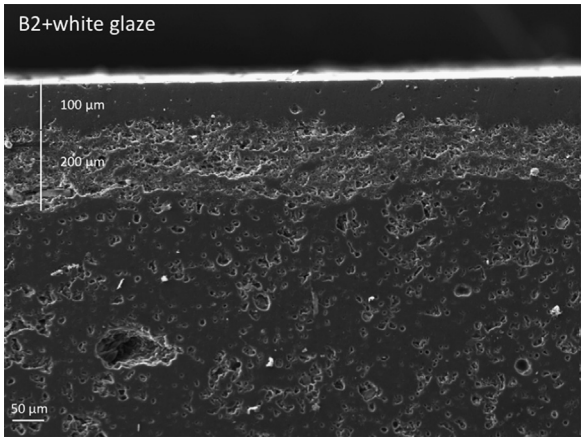


Fig. 5. Sample B2 and white gloss glaze cross section SED image 1000 × .

0.82, respectively (see Table 4 and Fig. 6). Samples with engobe formulation A2, on both red and white support, achieve good reflectance values as well, but the formulation was not considered for more investigation as it is very similar to B2. Samples with engobe formulation N2 also show good reflectance values, but the added raw material is relatively expensive and, therefore, they have been dropped in favor of cheaper engobes with similar or superior performance. It is interesting to highlight how these spectra does not decrease in Spectral Reflectivity with the increasing of wavelength, if compared with polymeric coatings [12]. The small variation on each spectrum in the 1900–2500 nm $\lambda$ is not outstanding, especially if we consider the small amount of solar spectral irradiance in that range.

In the second sample set (Set 2), a reduction of the solar reflectance values is generally observed between samples with similar compositions (see Table 4 and Fig. 7). The reason is the replacement of $ZrSiO_4$ by $TiO_2$ and, consequently, of the mineralogical phases added to the formulation. Samples with engobe compositions D2 and D3 present the lowest reflectance values, probably because the high glass percentage in the formulation (45 wt%) makes the engobes more vitreous.

In an industrial context it is important to apply an engobe with thickness providing an adequate effect but, at the same time, to achieve a good compromise on the amount of employed material. Therefore, different numbers of layers have been applied onto the same support to investigate the effect of the engobe thickness. Entering in detail, two, three and four layers of engobe were applied onto the red support. The selected formulation was that of sample B2, which reaches the best performance in terms of solar reflectance. The results, summarized in Table 5, show that an irrelevant increase of solar reflectance ($\rho_{sol}=0.01$) is obtained passing from one to two engobe layers, and that the same solar reflectance is practically obtained increasing the number of layers from two to three or four. Generally speaking, the thickness analysis shows that excellent levels of coverage can be reached, and just two engobe layers are enough to mask also a relatively dark (red) support and ensure the best performance.

The application of a vitreous glaze does not allow the samples to obtain the same performance of unglazed coupons,

although they can reach very good values of solar reflectance (Table 3). In this work, three glaze types where tested: transparent, glossy white, and matt white. Samples with transparent glaze are characterized by a smooth glossy and transparent surface, through which the color of the engobe below can be clearly seen. Samples with glossy white glaze have a smooth surface as well, but the glaze is opaque white and not transparent. Samples with matt white glaze, instead, show a smooth but matt surface, and it is impossible to see the engobe color because of the glaze.

Glazed samples with engobe composition C2, which is characterized by the presence of recycled glass in replacement of Na-feldspar, show solar reflectance values always lower than those for glazed samples with composition B2. For both compositions, a non-negligible drop of solar reflectance is observed with respect to the unglazed samples, showing that the glaze affects performance. Samples with engobe composition B2 and white gloss glaze seems to provide the highest reflectance values, as high as 0.85 on red support and 0.86 on white support. Transparent and white matt glazes, however, yields approximately the same results. As a comparison, white-colored clay or concrete tiles generally provide reflectance values between 0.60 and 0.75 [20]. Despite the decrease of $\rho_{sol}=0.04$ glazed samples are characterized by excellent solar performances and moreover enhanced mechanical properties.

Table 4
Solar reflectance of unglazed engobed samples in Set 1 and Set 2.

| $\rho_{sol}$ | Red support | White support |
|---|---|---|
| A2 | 0.80 | 0.82 |
| B2 | 0.90 | 0.90 |
| C2 | 0.81 | 0.82 |
| D2 | 0.65 | 0.70 |
| N2 | 0.79 | 0.81 |
| A3 | 0.70 | 0.72 |
| B3 | 0.81 | 0.81 |
| C3 | 0.73 | 0.74 |
| D3 | 0.63 | 0.66 |
| B2 (transparent) | 0.84 | 0.86 |
| B2 (glossy white) | 0.85 | 0.86 |
| B2 (matt white) | 0.84 | 0.86 |
| C2(transparent) | 0.78 | 0.81 |
| C2 (glossy white) | 0.82 | 0.83 |
| C2 (matt white) | 0.80 | 0.80 |

## 4. Conclusions

This work describes the procedure through which an engobe with high solar reflectance is obtained, using common production materials and processes of the ceramic tile industry. Two relatively inexpensive pigments were chosen to obtain a white engobe and one of them was selected after comparison of several formulations using both pigments. A solar reflectance of the engobe as high as 0.90 was obtained with either white or red ceramic support, with the chance to add one percent point by doubling the engobe thickness up to 200 μm.

In order to protect the engobe and improve its resistance to mechanical stress and weathering, the application of a glaze coating was subsequently investigated. Among the tested solutions, a white gloss glaze was found to give the best performance in terms of solar reflectance and functionality of the glazed tile, providing a white product with solar reflectance as high as 0.86 and the same predictable resistance to sun, rain and frost of ceramic tiles. On the other hand, a transparent gloss glaze was also produced with performance very close to that of the white gloss glaze. This can pave the way to the development of cool colored (i.e. non-white) tiles based on the same engobe and proper selective pigments added to the glaze.

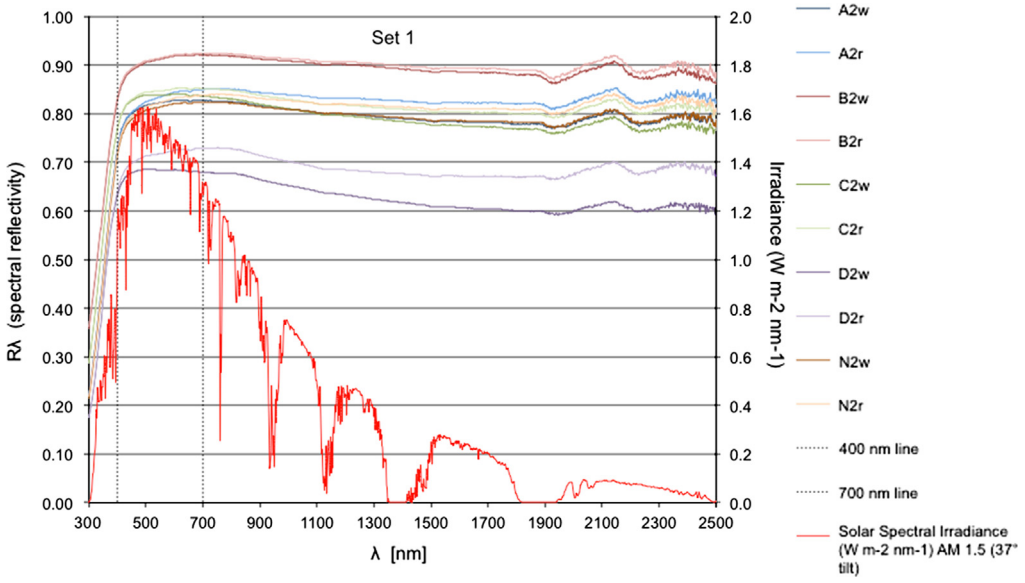


Fig. 6. Set 1 UV–vis–NiR spectra.

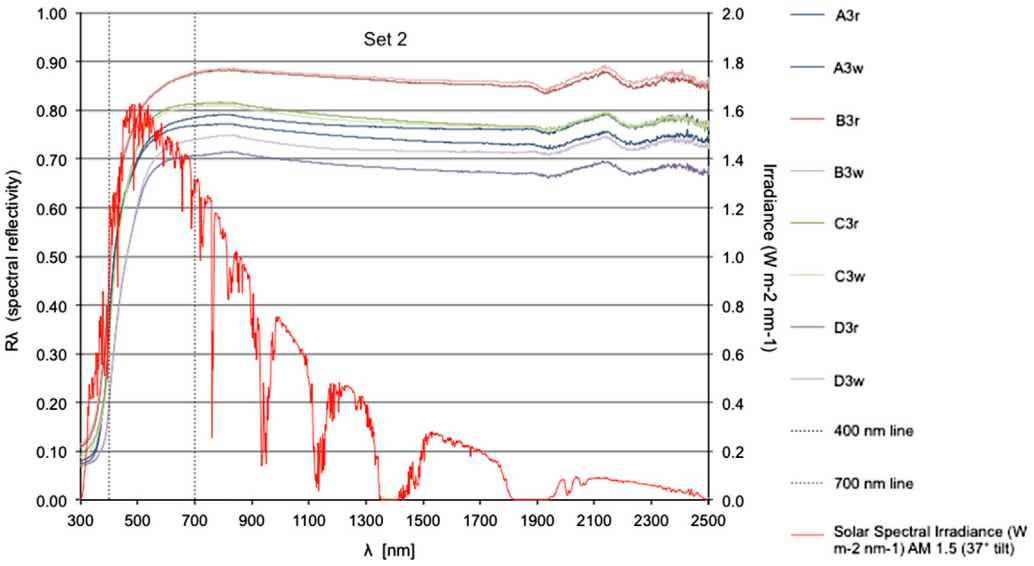


Fig. 7. Set 2 UV–vis–NiR spectra.

Table 5
Solar reflectance of unglazed samples with different engobe thickness.

| B2 (unglazed), support: layer number | Red $\rho_{sol}$ |
|---|---|
| 1 | 0.90 |
| 2 | 0.91 |
| 3 | 0.91 |
| 4 | 0.91 |

## Acknowledgments

The authors wish to thank Eng. Luca Rivi and the personnel of Intercolor, Sassuolo (Italy), for their technical collaboration and support.

This work was supported by InProCer Project (Laboratorio per l'innovazione di prodotto e processo ceramico Emilia Romagna, DGR no. 1631/2009 del 26 ottobre 2009) titled "Dai distretti Produttivi ai distretti tecnologici" ref. D.M. 28 dicembre 2007 "Progetti a favore dei distretti produttivi", art. 1, comma 890, L. 27 dicembre 2006 n. 296.

## References

[1] H. Akbari, H.D. Matthews, Global cooling updates: reflective roofs and pavements, Energy and Buildings 55 (2012) 2–6.
[2] M. Santamouris, Cooling the cities—a review of reflective and green roof mitigation technologies to fight heat island and improve comfort in urban environments, Solar Energy, http://dx.doi.org/10.1016/j.solener.2012.07.003, in press.
[3] H. Taha, H. Akbari, A. Rosenfeld, J. Huang, Residential cooling loads and the urban heat island—the effects of albedo, Building and Environment 23 (4) (1998) 271–283.
[4] H. Akbari, M. Pomerantz, H. Taha, Cool Surfaces and Shade Trees to Reduce Energy Use and Improve Air Quality in Urban Areas, Solar Energy 70 (3) (2001) 295–310.
[5] Z. Shi, X. Zhang, Analyzing the effect of the long wave emissivity and solar reflectance of building envelopes on energy-saving in buildings in various climates, Solar Energy 85 (1) (2011) 28–37.
[6] J.P. De Brito Filho, J.R. Henriquez, J.C.C. Dutra, Effects of coefficients of solar reflectivity and infrared emissivity on the temperature and heat flux of horizontal flat roofs of artificially conditioned nonresidential buildings, Energy and Buildings 43 (2–3) (2011) 440–445.
[7] A. Synnefa, M. Santamouris, Advances on technical, policy and market aspects of cool roof technology in europe: the cool roof project, Energy and Buildings 55 (2012) 35–41.
[8] R. Levinson, P. Berdahl, H Akbari, W. Miller, I. Joedicke, J. Reilly, Y. Suzuki, M. Vondran, Methods of creating solar-reflective nonwhite surfaces and their application to residential roofing materials, Solar Energy Materials and Solar Cells 91 (4) (2007) 304–314.
[9] A. Synnefa, M. Santamouris, K. Apostolakis, On the development, optical properties and thermal performance of cool colored coatings for the urban environment, Solar Energy 81 (4) (2007) 488–497.
[10] S. Kültür, N. Türkeri, Assessment of long term solar reflectance performance of roof coverings measured in laboratory and in field, Building and Environment 48 (2012) 164–172 February.
[11] A. Libbra, L. Tarozzi, A. Muscio, M.A. Corticelli, Spectral response data for development of cool coloured tile coverings, Optics and Laser Technology 43 (2) (2011) 394–400.
[12] A. Libbra, A. Muscio, C. Siligardi, P. Tartarini, Assessment and improvement of the performance of anti solar surfaces and coatings, Progress in Organic Coatings 72 (1–2) (2011) 73–80.
[13] R. Levinson, P. Berdahl, H. Akbari, Solar spectral optical properties of pigments—Part II: survey of common colorants, Solar Energy Materials and Solar Cells 89 (4) (2005) 351–389.
[14] T. Thongkanluang, T.P. Limsuwan, P. Rakkwamsuk, Preparation and application of high near-infrared reflective green pigment for ceramic tile roofs, International Journal of Applied Ceramic Technology 8 (6) (2011) 1451–1458.
[15] 2nd edition, Applied Ceramic Technology, vol. 1, La Mandragola, Bologna, Italy 139–174.
[16] I.Cer. S., Colore, Pigmenti e Colorazione in Ceramica, Editora S.A.L.A srl, Modena, Italia, 2003.
[17] ⟨http:/www.malvern.com/labeng/products/mastersizer/MS2000/mastersizer2000.htm⟩.
[18] E.P. Degarmo, J.T. Black, R.A. Kohser, 9th edition, Materials and Processes in Manufacturing, 223, John Wiley & Sons, 2003.
[19] W.M. Carty, U. Senapati, Porcelain—raw materials, processing, phase evolution, and mechanical behavior, Journal of the American Ceramic Society 81 (1998) 3–20.
[20] M. Santamouris, A. Synnefa, T. Karlessi, Using advanced cool materials in the urban built environment to mitigate heat islands and improve thermal comfort conditions, Solar Energy 85 (12) (2011) 3085–3102.